Control of coherent backscattering by breaking optical reciprocity

Y. Bromberg,* B. Redding, S. M. Popoff,† and H. Cao‡
Department of Applied Physics, Yale University, New Haven, Connecticut 06520, USA
(Received 16 May 2015; revised manuscript received 15 November 2015; published 18 February 2016)

Reciprocity is a universal principle that has a profound impact on many areas of physics. A fundamental phenomenon in condensed-matter physics, optical physics, and acoustics, arising from reciprocity, is the constructive interference of quantum or classical waves which propagate along time-reversed paths in disordered media, leading to, for example, weak localization and metal-insulator transition. Previous studies have shown that such coherent effects are suppressed when reciprocity is broken. Here we experimentally show that by tuning a nonreciprocal phase we can coherently control complex coherent phenomena, rather than simply suppress them. In particular, we manipulate coherent backscattering of light, also known as weak localization. By utilizing a magneto-optical effect, we control the interference between time-reversed paths inside a multimode fiber with strong mode mixing, observe the optical analog of weak antilocalization, and realize a continuous transition from weak localization to weak antilocalization. Our results may open new possibilities for coherent control of waves in complex systems.

DOI: 10.1103/PhysRevA.93.023826

I. INTRODUCTION

The reciprocity principle demands that waves which propagate along time-reversed paths exhibit the exact same transmission, no matter how complex the paths are [1]. It has profound and often surprising implications regarding the transport of classical and quantum waves in complex systems as it poses a symmetry that is not distorted by disorder. When pairs of time-reversed paths interfere, reciprocity guarantees that the interference is constructive for any realization of disorder [Fig. 1(a)]. This robust interference is the underlying mechanism of weak localization, a coherent correction to incoherent transport models, such as the Drude-Boltzmann for electrical conductance and the radiative transfer equation for light [2]. The discovery of weak localization, originally for mesoscopic transport of electrons, marked a milestone in the research of complex coherent phenomena [3]. It established the importance of interference effects even when waves are randomly scattered, eventually leading to the celebrated strong (Anderson) localization. In optics, weak localization is manifested by an enhancement by a factor of 2 of the backscattered intensity, an effect coined coherent backscattering (CBS) [4–7].

The role of reciprocity in multiple scattering phenomena is elucidated when it is broken. For electrons, reciprocity is broken by magnetic fields that induce Aharonov-Bohm oscillations recorded by magnetoresistance measurements [8,9]. For matter waves, suppression and revival of CBS were recently observed by applying an instantaneous dephasing kick to a cloud of ultracold atoms [10]. The suppression of CBS under time-reversal symmetry breaking was also demonstrated with acoustic waves in a rotating medium [11]. In optics, previous studies on broken reciprocity with magneto-optical effects [12] or nonlinearity [13] in scattering systems showed suppression of the CBS enhancement: Individual pairs of time-reversed paths acquire a random relative phase, resulting in an incoherent suppression of CBS [14,15]. Here, we demonstrate a scheme for a precise tuning of the nonreciprocal phase between all pairs of time-reversed paths, which enables control of the CBS by maintaining the coherence. Specifically, we observe the optical analog of weak antilocalization [3], manifested by a dip in the backscattered intensity. We further demonstrate a continuous transition from a CBS peak (weak localization) to a CBS dip (weak antilocalization). We thus diversify the CBS phenomenon, showing that coherent backscattering is not necessarily associated with enhancement of the backscattered intensity but can exhibit richer behavior.

Since optical reciprocity and specifically CBS are universal phenomena, they can be studied in a wide range of scattering systems, such as paints, colloids, and biological tissue. Here we study CBS in multimode optical fibers with strong mode mixing. In recent years there has been an increasing interest in exploiting multimode fibers for numerous applications, including optical communication [16], imaging [17,18], and spectroscopy [19]. Multimode fibers and fiber bundles were also used for fundamental studies of mesoscopic transport in disordered media [20–22]. In this paper, we wish to control light transport in disordered media. To this end, we take two unique advantages of fibers over scattering samples. First, the transmission through the fiber is extremely high, even in the presence of strong mode mixing, and thus information of the input state of the light is only scrambled but not lost. This is in contrast to multiple scattering (diffusive) samples where most of the incident light is reflected. Second, unlike random scattering samples, fibers allow to fully control the coupling of the input light to all the guided modes, thanks to the finite numerical aperture. In this paper, we utilize these properties of fibers to control CBS.

II. RESULTS

Unlike scattering media, in optical fibers backscattering is negligible. However, we can take advantage of the versatility

*Current address: Racah Institute of Physics, The Hebrew University of Jerusalem, Jerusalem 91904, Israel.
†Current address: CNRS - LTCI Télécom ParisTech, 46 rue Barrault, 75013 Paris, France.
‡Corresponding author: hui.cao@yale.edu

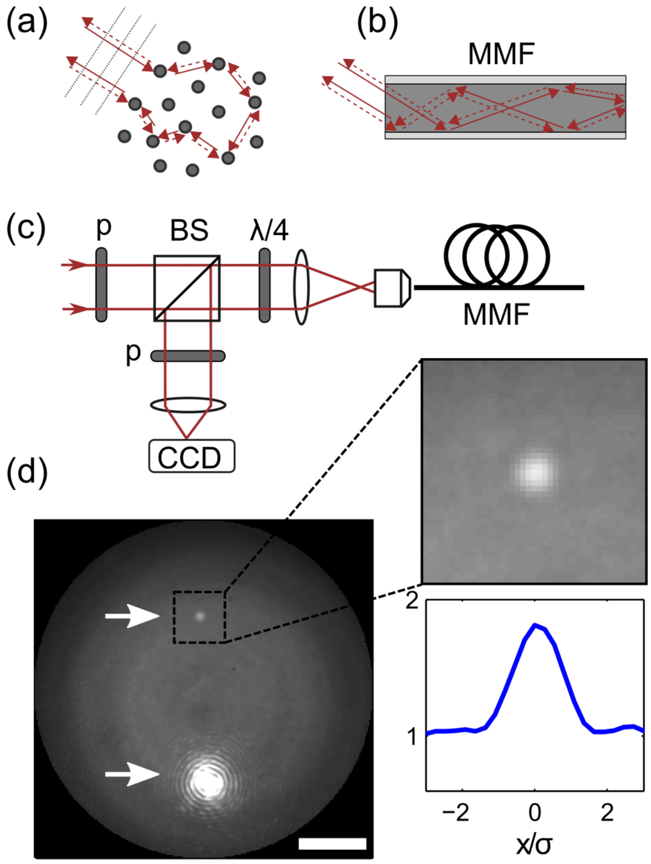

FIG. 1. Coherent backscattering of light in a multimode fiber (MMF). (a) Illustration of CBS in a random scattering sample, depicting one pair of time-reversed paths (solid and dashed arrows). The two paths accumulate the same phase inside the sample and interfere constructively in the direction opposite from the incident wave. (b) Illustration of CBS in a MMF. Due to fiber imperfections, twisting, and bending, the guided modes are strongly coupled, and the light can propagate through many different paths. Part of the light is backreflected from the output end of the fiber due to Fresnel reflection, creating time-reversed paths as illustrated. (c) Schematic of the experimental setup for observing CBS in a MMF. A laser beam ($\lambda = 640$ nm) is coupled to a 5-m-long step-index multimode fiber that supports ∼1500 guided modes. The incident beam is collimated, and its direction deviates from the normal of the input facet of the fiber so that the backscattering direction differs from that of the specular reflection. The backreflected light is picked up with a beam splitter (BS) and recorded by a CCD camera. An additional lens is used to image the far field of the fiber front facet to the camera. The light impinging on the fiber is circularly polarized to suppress specular reflection from the front facet of the fiber (p—linear polarizer and λ/4—quarter-wave plate). The linear polarizer is placed in front of the camera to detect light in the same polarization as the input (co-polarization channel). (d) Far field intensity distribution of the returning light, averaged over 200 fiber configurations. Enhanced intensity in the backscattering direction is observed (top arrow) and in its mirrored position is a strong specular reflection (bottom arrow). The insets show a magnified view of the CBS peak and a cross section of the averaged intensity with an enhancement factor of 1.81. The scale bar represents 0.05 rad. $\sigma = 0.004$ rad is the full width at half maximum of a single speckle grain.

of fibers to study CBS in diverse configurations. We start with the simplest configuration, a double passage configuration where due to the Fresnel reflection at the output facet of the fiber, light which propagates through the fiber can be reflected back towards the input facet. Thus, constructive interference of light which propagates along time-reversed paths becomes possible [Fig. 1(b)]. Due to the strong mode mixing, after the light propagates back to the input facet, it exhibits a random grainy pattern called speckle, which resembles the pattern formed by light that is backscattered from random scattering. We therefore refer to the light coming back from the fiber as backscattered light, similar to the terminology used for double passage through distorting phase screens [23–25]. Accordingly, we consider the coherent enhancement as coherent backscattering.

As in typical CBS experiments with scattering samples, to maximize the CBS enhancement we illuminated the fiber with a well-defined incident angle [26], detected the light at the far field of the fiber facet, and measured the co-polarization channel [Fig. 1(c), see also Methods]. The fiber was a 5-m-long step-index multimode fiber which supports ∼1500 guided modes. The guided modes were strongly coupled due to fiber imperfections and stress induced by bending the fiber. The interference between the guided modes results in a speckle pattern that is measured by a CCD camera. After averaging over 200 distinct speckle patterns that were recorded while the fiber was constantly perturbed, a smooth intensity distribution was obtained [Fig. 1(d)]. The average intensity exhibits two bright regions: a saturated spot (bottom arrow) due to the specular reflection from the front facet and the CBS signal (top arrow). The two bright regions are separated because we tilted the fiber facet relative to the angle of the input beam. Similar to phase conjugation [27], the CBS is observed exactly in the opposite direction from the input beam, whereas the specular reflection is observed at the mirrored position. The width of the CBS enhancement area is determined by the diffraction limit, i.e., it is equal to the average width of a single speckle grain. It is inversely proportional to the diameter of the fiber core and does not depend on the fiber length or on the strength of the disorder. In fact, since the enhancement originates from the reciprocity principle, it can be observed also in a perfectly straight fiber without any mode mixing, provided that several guided modes of the fiber are excited by the input light. The key point is that the effect is robust to the disorder in the fiber.

The above example shows that CBS exists in multimode fibers in a double passage setting that resembles CBS in scattering media. In the following, we studied CBS in a new configuration, which takes advantage of the high transmission through fibers. Specifically we investigated whether the light that is transmitted through the fiber can also exhibit interference between time-reversed paths. To this end, we injected light to both ends of the fiber by splitting the input beam by a beam splitter [BS1 in Fig. 2(a)]. The counterpropagating fields inside the fiber were combined by BS1, forming a Sagnac loop. The light can propagate through many different paths inside the fiber, yet for every path that propagates in the clockwise direction, there is a reciprocal path that propagates in the counterclockwise direction. Every pair of reciprocal paths accumulates the same phase. Thus, when measuring

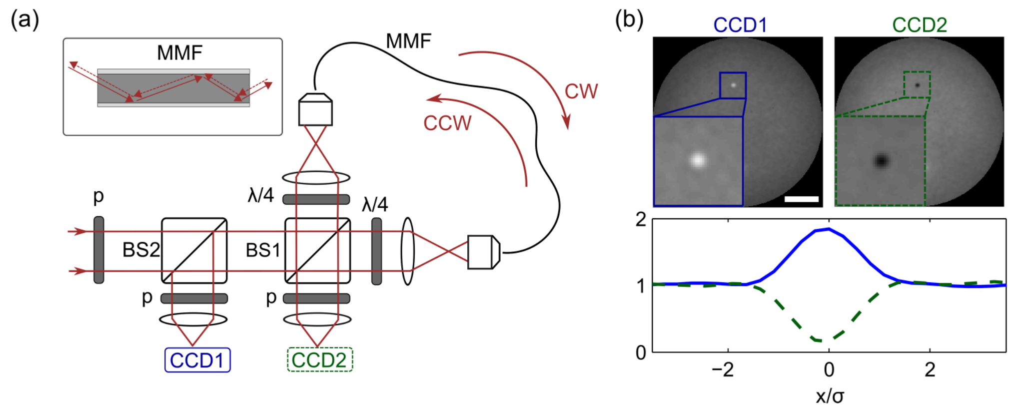

FIG. 2. Coherent backscattering in a MMF loop. (a) A collimated laser beam is split by BS1 and coupled to the two end facets of a 6-m-long step-index multimode fiber. The transmitted fields are recombined by BS1, forming a Sagnac loop. The two facets of the fiber are positioned at conjugated planes, and their combined far field images are recorded by CCD1 and CCD2. The inset shows an illustration of one pair of counterpropagating paths in the fiber. (b) Top panel: images recorded by the two cameras, averaged over 200 configurations of the fiber. On CCD1 a CBS peak is observed due to constructive interference of time-reversed paths, and on CCD2 a CBS dip is observed due to destructive interference. Since the illumination and detection channels are at different ports of BS1, the destructive interference in CCD2 does not violate the reciprocity principle. Bottom panel: intensity distribution in the vicinity of the backscattering direction (CCD1: blue solid line; CCD2: green dashed line). The CBS peak to background ratio is 1.85, and the dip to background ratio is 0.15. The scale bar represents 0.05 rad. $\sigma = 0.004$ rad is the full width at half maximum of a single speckle grain.

the co-polarization channel, the two counterpropagating fields interfere constructively on a camera which images the light that propagates back towards the source (CCD1), resulting in a CBS peak in Fig. 2(b).

Interestingly, the loop configuration also allows us to observe a destructive interference between time-reversed paths by recording the light that exits from the second port of BS1 (CCD2). A dip, rather than a peak, was then observed. This, however, does not indicate that reciprocity was broken. Since the illumination and detection were performed at different ports of BS1, strictly speaking this is not a CBS configuration. The mechanism for the destructive interference is the phase shift associated with reflection and transmission by lossless beam splitters: Since the counterclockwise paths are reflected twice by BS1 and the clockwise paths are transmitted twice, they accumulate a π phase shift [28]. We note that to identify a region of perfect destructive interference requires averaging over just a few speckle realizations. Despite speckle variation from one realization to another, the destructive interference between the two paths always produces a null intensity at the same position, whereas the locations of other null intensities due to interference of many random paths would vary with realizations, and the probability to detect a null intensity for a sum of even just two uncorrelated speckle patterns is negligible. In contrast, to observe a CBS peak it is necessary to average over many more realizations since the intensity measured at the peak position fluctuates between realizations.

Next, we show that it is possible to control CBS, by tuning the relative phase between the time-reversed paths in the multimode fiber. It is well known that in systems with a single spatial mode, this phase can be controlled using a nonreciprocal mechanism, such as the magneto-optical effect, or fast temporal modulations, which were used for example to demonstrate the photonic Aharonov-Bohm effect [29,30]. However, in multiple scattering systems, broken reciprocity typically results in the suppression of coherent effects and specifically the suppression of CBS [12,13,15]. The reason is that in disordered multimode systems, different pairs of time-reversed paths accumulate different nonreciprocal phases, and the superposition of all the pairs smears out interference effects. This happened in scattering media with a strong magneto-optical response where different paths encountered a different overlap with the magnetic field [12]. However, multimode fibers allow the same nonreciprocal phase to be imposed on all pairs of time-reversed paths. We achieved this by adding a Faraday rotator to the Sagnac interferometer, a configuration which was previously considered for optical switches [31]. A Faraday rotator is composed of a magnetic-optical crystal and a permanent magnet producing a magnetic field that is orientated along the propagation direction. It introduces opposite phase delays for right and left circularly polarized light. The magnitude of the phase delay depends on the strength of the magnetic field, on the angle between the magnetic field, and on the propagation direction. Most importantly, reciprocity is broken because the phase delay for light with the same circular polarization has opposite signs when the propagation direction is parallel or antiparallel to the magnetic field.

We placed the Faraday rotator in between two segments of the multimode fiber (5-m and 1-m long) and added a collimating lens on each side of the rotator [Fig. 3(a)]. The beam coming out of the fiber was therefore nearly collimated when passing through the rotator, and thus the angle between the magnetic field and the propagation direction for each of the paths through the rotator was approximately the same. This does not mean that all the paths experience the same nonreciprocal phase. The strong mode mixing in our multimode fiber completely scrambles the polarization of the light, thus at the input surface of the Faraday rotator, the polarization state of each path has a different composition of the left and right circular polarization components. Since the two circular polarizations acquire an opposite phase inside the

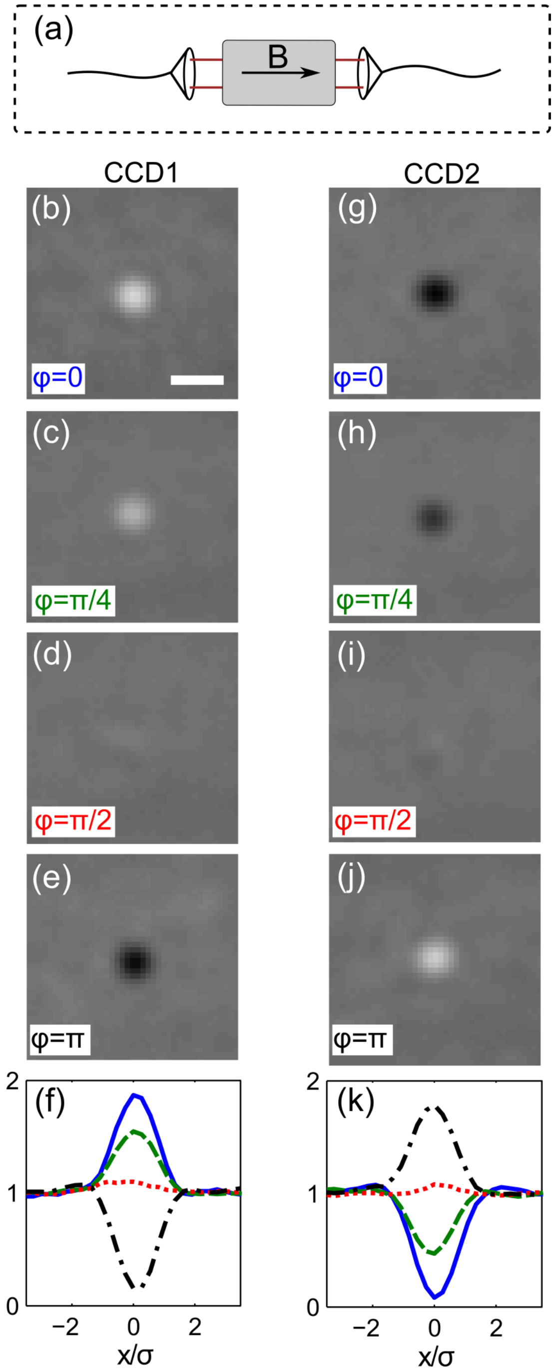

FIG. 3. Control of coherent backscattering with a Faraday rotator. (a) A Faraday rotator is inserted to the fiber loop shown in Fig. 2 by splitting the multimode fiber to two segments (5-m and 1-m long) and placing the Faraday rotator in between. Two collimators are placed on both sides of the Faraday rotator to collimate the beams coming out of the fiber and refocusing them into the other fiber. (b)–(e) Magnified view of the CBS signal measured by CCD1 for four nonreciprocal phases φ induced by the Faraday rotator. (b) $\varphi = 0$, (c) $\pi/4$, (d) $\pi/2$, and (e) π. The scale bar represents 0.01 rad. A continuous transition is observed from a CBS peak (peak to background ratio of 1.86) to a dip (dip to background ratio of 0.15). (f) Cross sections of the images (b)–(e) ($\varphi = 0$ blue solid line, $\varphi = \pi/4$ green dashed line, $\varphi = \pi/2$ red dotted line, and $\varphi = \pi$ black dashed-dotted line). $\sigma = 0.004$ rad is the full width at half maximum of a single speckle grain. (g)–(k): The same as (b)–(f) for the images recorded by CCD2.

Faraday rotator, the net effect is path dependent. Nevertheless, the nonreciprocal effect is insensitive to the polarization scrambling and is not washed out upon ensemble averaging. The reason is that for each pair of time-reversed paths, the circular polarization decomposition is identical at the input of the rotator. For example, if the Faraday rotator imposes a phase of $\varphi/2$ on the right circular polarized light propagating in the clockwise direction, it will impose a phase of $-\varphi/2$ on the right circular polarized light propagating in the counterclockwise direction. Then for each pair of time-reversed paths the phase *difference* between the clockwise and the counterclockwise paths is φ for the right circular polarization component and $-\varphi$ for the left circular polarization component. Hence, regardless of the polarization decomposition of the polarization state at the input of the Faraday rotator, the interference between each pair of time-reversed paths produces the same $\cos(\varphi)$ modulation of backscattered intensity.

By adjusting the distance between the crystal and the permanent magnet, we controlled the effective strength of the magneto-optical effect and tuned the nonreciprocal phase φ. Figure 3 depicts the average intensities recorded by the cameras CCD1 and CCD2 for different values of the nonreciprocal phase φ, applied by the Faraday rotator. The CBS peak on CCD1 (with the peak to background ratio of 1.86) turns into a dip (with the dip to background ratio of 0.15) at $\varphi = \pi$. Similarly, the dip on CCD2 turns into a peak. This transition, the optical analog of the weak localization and weak antilocalization crossover [32], demonstrates that the interference between reciprocal paths inside the fiber can be continuously tuned from constructive to destructive with a visibility of 85%. In contrast to the wave-front shaping approach for controlling light in multimode optical fibers [18,33,34], our method of CBS control is robust against fluctuations in the configuration of the fiber or in its environmental conditions.

III. DISCUSSION

In this paper, we demonstrated two mechanisms for observing robust destructive interference between pairs of counterpropagating paths inside the multimode fiber. In the first demonstration, the destructive interference was possible without breaking reciprocity because the extra port of the beam splitter provided access to returning light in a final state that is orthogonal to the input state. Similarly, a CBS dip without breaking reciprocity was observed for acoustic waves by placing the source and detector at different locations inside a cavity [35]. For electrons, weak antilocalization without breaking reciprocity was observed in thin metallic films [3,36] and in quantum dots [37] with strong spin-orbit coupling which causes the spin of the output state to be antiparallel to the spin of the input state. A related effect was observed in graphene where rotation of the pseudospin along the propagation path also results in weak antilocalization [38]. In optics, it was predicted that in photonic graphene lattices, the pseudospin of the backscattered wave is antiparallel to the input pseudospin direction, resulting in a CBS dip due to a Berry phase of π [39]. Consequently, enhanced transmission in photonic graphene lattices was observed in the microwave regime [40]. Here, we directly measured the destructive interference between the counterpropagating paths inside the fiber.

It is instructive to compare the CBS peak in the double passage configuration (Fig. 1) to previous works on phase conjugation in multimode fibers using nonlinear crystals placed at the distal end of the fiber [27,41,42]. In contrast to optical phase conjugation, the CBS peak results from the reflection from the distal end of the fiber due to index mismatch, and it is therefore a robust effect. However, since in CBS only pairs of time-reversed paths interfere constructively, the ratio of the CBS peak to the background is limited to 2, whereas the phase conjugation makes all the light backreflected to the direction opposite to the input beam.

In the second approach, we broke reciprocity in order to observe the CBS dip, i.e., the destructive interference was between strictly time-reversed paths. Reciprocity breaking mechanisms for obtaining a CBS dip were only theoretically proposed before, e.g., for scattering of light from ultracold atoms where reciprocity was broken either by the magnetic field and Zeeman splitting [43] or by nonlinear light-matter interactions [44,45]. Our approach using a magneto-optical effect, allows not only a direct observation of the CBS dip, but also a precise control of the relative phase between the time-reversed paths. We demonstrated a continuous transition from a CBS peak to a dip with a visibility that is orders of magnitude larger than the visibility of the oscillations in magnetoresistance measurements of electrons subject to a nonreciprocal Aharonov-Bohm phase [8,9].

In conclusion, we developed a configuration for coherently manipulating the nonreciprocal phase and interference between time-reversed paths and demonstrated a precise control that is robust against external perturbations. In particular, we observed the optical analog of weak antilocalization and the transition from weak localization to antilocalization. The approach presented here can be used to study a wide range of complex coherent phenomena with broken reciprocity. For example, since CBS is often considered the precursor of Anderson localization, an intriguing question is how the destructive interference of time-reversed paths will affect the mesoscopic transport of light in complex systems, and specifically how it will impact strong localization. By constructing a complex network of multimode fibers and Faraday rotators, we now have experimental means to investigate such questions. Moreover, our approach for precise tuning of the nonreciprocal phase can readily be adapted to other configurations that were already used for studying Anderson localization of light [46] and may create new physical phenomena. In addition, multimode fibers can further provide exceptional opportunities for increasing the complexity of the system through optical nonlinearities [47] or by using chaotic fibers [48]. These aspects are also expected to have practical implications for sensing, imaging, and communication applications that are based on multimode fibers.

IV. METHODS

CBS setup. We spatially filtered a linearly polarized cw laser beam ($\lambda = 640$ nm, OBIS LX, Coherent) and clipped it with an iris to create a nearly flattop beam. We then coupled the beam to the multimode fiber by demagnifying it using a lens and a microscope objective ($\times 20$, numerical aperture $= 0.4$). The beam at the input facet slightly overfilled the core of the fiber (diameter $D = 105\,\mu$m). To separate the specular reflection from the CBS signal we tilted the facet of the fiber. The returning light was collected with the same objective, and the back focal plane of the objective was reimaged onto the CCD camera, i.e., we recorded the Fourier plane of the fiber facet. We used a linear polarizer in front of the CCD camera to measure the same polarization as the incident beam (i.e., co-polarization channel). We placed a quarter-wave plate before the fiber, orientated at 45° relative to the incident polarization direction, in order to reduce the specular reflection from the input facet of the fiber. The above setting was used for the double passage and the Sagnac configurations.

Multimode fiber. In all the configurations we studied, we used a standard step-index multimode fiber with a numerical aperture of 0.22 and a core diameter of 105 μm. We twisted and bent the fiber to enhance mode mixing. All our measurements were performed in the regime of strong mode mixing, which created a homogenous distribution of the ensemble-averaged intensity at the far field of the fiber facet.

ACKNOWLEDGMENTS

We thank D. Stone, D. Prober, and S. Fan for fruitful discussions. We acknowledge support from the National Science Foundation under Grant No. DMR-1205307 and the US Office of Naval Research under MURI Grant No. N00014-13-1-0649.

[1] D. Jalas *et al.*, What Is—and What Is Not—an Optical Isolator, Nat. Photonics **7**, 579 (2013).
[2] E. Akkermans and G. Montambaux, *Mesoscopic Physics of Electrons and Photons* (Cambridge University Press, Cambridge, UK, 2007).
[3] G. Bergmann, Weak localization in thin films: A time-of-flight experiment with conduction electrons, Phys. Rep. **107**, 1 (1984).
[4] Y. Kuga and A. Ishimaru, Retroreflectance from a dense distribution of spherical particles, J. Opt. Soc. Am. A **1**, 831 (1984).
[5] M. P. Van Albada and A. Lagendijk, Observation of Weak Localization of Light in a Random Medium, Phys. Rev. Lett. **55**, 2692 (1985).
[6] P.-E. Wolf and G. Maret, Weak Localization and Coherent Backscattering of Photons in Disordered Media, Phys. Rev. Lett. **55**, 2696 (1985).
[7] E. Akkermans, P. E. Wolf, and R. Maynard, Coherent Backscattering of Light by Disordered Media: Analysis of the Peak Line Shape, Phys. Rev. Lett. **56**, 1471 (1986).
[8] D. Y. Sharvin and Y. V. Sharvin, Quantization in a cylindrical film of a normal metal, Pis'ma Zh. Eksp. Teor. Fiz. **34**, 285 (1981) [JETP Lett. **34**, 272 (1981)].
[9] V. Chandrasekhar, M. J. Rooks, S. Wind, and D. E. Prober, Observation of Aharonov-Bohm Electron Interference Effects with Periods h/e and h/2e in Individual Micron-Size, Normal-Metal Rings, Phys. Rev. Lett. **55**, 1610 (1985).

[10] K. Müller, J. Richard, V. V. Volchkov, V. Denechaud, P. Bouyer, A. Aspect, and V. Josse, Suppression and Revival of Weak Localization through Control of Time-Reversal Symmetry, Phys. Rev. Lett. **114**, 205301(2015).
[11] J. de Rosny, A. Tourin, A. Derode, P. Roux, and M. Fink, Weak Localization and Time Reversal of Ultrasound in a Rotational Flow, Phys. Rev. Lett. **95**, 074301 (2005).
[12] F. Erbacher, R. Lenke, and G. Maret, Multiple light scattering in magneto-optically active media, Europhys. Lett. **21**, 551 (1993).
[13] O. L. Muskens, P. Venn, T. van der Beek, and T. Wellens, Partial Nonlinear Reciprocity Breaking through Ultrafast Dynamics in a Random Photonic Medium, Phys. Rev. Lett. **108**, 223906 (2012).
[14] F. C. MacKintosh and S. John, Coherent backscattering of light in the presence of time- reversal- noninvariant and parity-nonconserving media, Phys. Rev. B **37**, 1884 (1988).
[15] D. S. Wiersma, Light transport: Breaking reciprocity, Nat. Photonics **6**, 506 (2012).
[16] S. Ö. Arik, J. M. Kahn, and K. P. Ho, MIMO signal processing for mode-division multiplexing: An overview of channel models and signal processing architectures, IEEE Signal Process Mag. **31**, 25 (2014).
[17] Y. Choi, C. Yoon, M. Kim, T. D. Yang, C. Fang-Yen, R. R. Dasari, K. J. Lee, and W. Choi, Scanner-Free and Wide-Field Endoscopic Imaging by Using a Single Multimode Optical Fiber, Phys. Rev. Lett. **109**, 203901 (2012).
[18] T. Cižmár and K. Dholakia, Exploiting multimode waveguides for pure fibre-based imaging, Nat. Commun. **3**, 1027 (2012).
[19] B. Redding, M. Alam, M. Seifert, and H. Cao, High-resolution and broadband all-fiber spectrometers, Optica **1**, 175 (2014).
[20] T. Pertsch, U. Peschel, J. Kobelke, K. Schuster, H. Bartelt, S. Nolte, A. Tünnermann, and F. Lederer, Nonlinearity and Disorder in Fiber Arrays, Phys. Rev. Lett. **93**, 053901 (2004).
[21] S. Karbasi, R. J. Frazier, K. W. Koch, T. Hawkins, J. Ballato, and A. Mafi, Image transport through a disordered optical fibre mediated by transverse anderson localization, Nat. Commun. **5**, 3362 (2014).
[22] M. Leonetti, S. Karbasi, A. Mafi, and C. Conti, Observation of Migrating Transverse Anderson Localizations of Light in Nonlocal Media, Phys. Rev. Lett. **112**, 193902 (2014).
[23] Y. A. Kravtsov and A. I. Saichev, Effects of double passage of waves in randomly inhomogeneous media, Sov. Phys. Usp. **25**, 494 (1982).
[24] P. R. Tapster, A. R. Weeks, and E. Jakeman, Observation of backscattering enhancement through atmospheric phase screens, J. Opt. Soc. Am. A **6**, 517 (1989).
[25] C. Schwartz and A. Dogariu, Enhanced backscattering of optical vortex fields, Opt. Lett. **30**, 1431 (2005).
[26] A. Dogariu and G. D. Boreman, Enhanced backscattering in a converging-beam configuration, Opt. Lett. **21**, 1718 (1996).
[27] A. Yariv, Y. Tomita, and K. Kyuma, Theoretical model for modal dispersal of polarization information and its recovery by phase conjugation, Opt. Lett. **11**, 809 (1986).
[28] A. Zeilinger, General properties of lossless beam splitters in interferometry, Am. J. Phys. **49**, 882 (1981).
[29] K. Fang, Z. Yu, and S. Fan, Photonic Aharonov-Bohm Effect Based on Dynamic Modulation, Phys. Rev. Lett. **108**, 153901 (2012).
[30] L. D. Tzuang, K. Fang, P. Nussenzveig, S. Fan, and M. Lipson, Non-reciprocal phase shift induced by an effective magnetic flux for light, Nat. Photonics **8**, 701 (2014).
[31] S. Kemmet, M. Mina, and R. J. Weber, Sagnac interferometric switch utilizing faraday rotation, J. Appl. Phys. **105**, 07E702 (2009).
[32] M. Liu *et al.*, Crossover between Weak Antilocalization and Weak Localization in a Magnetically Doped Topological Insulator, Phys. Rev. Lett. **108**, 036805 (2012).
[33] I. N. Papadopoulos, S. Farahi, C. Moser, and D. Psaltis, Focusing and scanning light through a multimode optical fiber using digital phase conjugation, Opt. Express **20**, 10583 (2012).
[34] L. V. Amitonova, A. P. Mosk, and P. W. H. Pinkse, The rotational memory effect of a multimode fiber, Opt. Express **23**, 20569 (2015).
[35] T. Gallot, C. Stefan, and P. Roux, Coherent backscattering enhancement in cavities: Highlight of the role of symmetry, J. Acoust. Soc. Am. **128**, 2314 (2010).
[36] S. Hikami, A. Larkin, and Y. Nagaoka, Spin-orbit interaction and magnetoresistance in the two dimensional random system, Prog. Theor. Phys. **63**, 707 (1980).
[37] D. M. Zumbühl, J. B. Miller, C. M. Marcus, K. Campman, and A. C. Gossard, Spin-Orbit Coupling, Antilocalization, and Parallel Magnetic Fields in Quantum Dots, Phys. Rev. Lett. **89**, 276803 (2002).
[38] F. V. Tikhonenko, A. A. Kozikov, A. K. Savchenko, and R. V. Gorbachev, Transition between Electron Localization and Antilocalization in Graphene, Phys. Rev. Lett. **103**, 226801 (2009).
[39] R. A. Sepkhanov, A. Ossipov, and C. W. J. Beenakker, Extinction of coherent backscattering by a disordered photonic crystal with a dirac spectrum, Europhys. Lett. **85**, 14005 (2009).
[40] X. Wang, H. T. Jiang, C. Yan, Y. Sun, Y. H. Li, Y. L. Shi, and H. Chen, Anomalous transmission of disordered photonic graphenes at the dirac point, Europhys. Lett. **103**, 17003 (2013).
[41] A. Yariv, Three-dimensional pictorial transmission in optical fibers, Appl. Phys. Lett. **28**, 88 (1976).
[42] B. Fischer and S. Sternklar, Image transmission and interferometry with multimode fibers using self-pumped phase conjugation, Appl. Phys. Lett. **46**, 113 (1985).
[43] D. V. Kupriyanov, I. M. Sokolov, and M. D. Havey, Antilocalization in coherent backscattering of light in a multi-resonance atomic system, Opt. Commun. **243**, 165 (2004).
[44] V. M. Agranovich and V. E. Kravtsov, Nonlinear backscattering from opaque media, Phys. Rev. B **43**, 13691(R) (1991).
[45] B. Grémaud and T. Wellens, Speckle Instability: Coherent Effects in Nonlinear Disordered Media, Phys. Rev. Lett. **104**, 133901 (2010).
[46] M. Segev, Y. Silberberg, and D. N. Christodoulides, Anderson localization of light, Nat. Photonics **7**, 197 (2013).
[47] L. G. Wright, D. N. Christodoulides, and F. W. Wise, Controllable spatiotemporal nonlinear effects in multimode fibres, Nat. Photonics **9**, 306 (2015).
[48] V. Doya, O. Legrand, F. Mortessagne, and C. Miniatura, Light Scarring in an Optical Fiber, Phys. Rev. Lett. **88**, 014102 (2001).